Biophysical Chemistry 151 (2010) 86–90

Contents lists available at ScienceDirect

Biophysical Chemistry

journal homepage: http://www.elsevier.com/locate/biophyschem

Short communication

Characterizing the denatured state of human prion 121–230

Cheng-I Lee *, Nai-yuan Chang

Department of Life Science, National Chung Cheng University, Ming-Hsiung, Chia-Yi 62102, Taiwan, ROC

ARTICLE INFO

Article history:
Received 17 March 2010
Received in revised form 6 May 2010
Accepted 8 May 2010
Available online 15 May 2010

Keywords:
Denatured state
Human prion
Self-guided Langevin dynamics

ABSTRACT

Misfolding and aggregation of the prion protein (PrP) are responsible for the development of fatal transmissible neurodegenerative diseases. PrP undergoes structural conversion from a natively folded state into a misfolded state, resulting in insoluble amyloid fibrils. Partial unfolding has been recognized as an essential step in fibrillation. The strong correlation of unfolding and fibrillation emphasizes the importance of denatured states. To gain insight into possible aggregation-prone denatured states, we characterized the denatured state of human prion (huPrP) 121–230 near extended conformation by self-guided Langevin dynamics simulations. Our results revealed that denatured huPrP is partially folded with α-helical structure.

1. Introduction

The denatured state has traditionally been considered an unfolded state with a lack of ordered structures. In the early 1990s, the denatured state has drawn extensive attention in the study of protein folding since the conservation of residual structures in the denatured states was identified [1]. Subsequent studies indicated that the residual structures of the denatured state are important in modulating the folding rates and early folding events [2,3]. Recent experimental studies have characterized the denatured state structure in great detail, and found that the denatured states have residual native secondary structures and sometimes even partial native tertiary structures [4,5]. Unlike the native state, the denatured state is typically populated with an ensemble of diverse structures [6], referred to as denatured state ensembles (DSE). The structural features presented in DSE are clearly linked to the folding process. A full clarification of protein folding mechanisms requires a comprehensive understanding of these features and their roles in protein folding. However, due to the structural diversity and the mobility of DSE, characterization of DSE is a significant challenge in view of current experimental approaches.

Prion proteins (PrPs) are infectious pathogens of a group of fatal neurodegenerative disease in mammalians known as transmissible spongiform encephalopathies (TSEs) [7]. TSEs can be ascribed to conformational conversion of prion. The normal, cellular form of PrP (PrP^C) is rich in α-helix structures, whereas the abnormal and infectious, Scrapie isoform of PrP (PrP^{Sc}) has a pronounced tendency to misfold and to aggregate subsequently into highly stable and insoluble plaques rich with β-sheet structures. The structure of PrP^{Sc} and mechanism of its formation have not yet been fully elucidated.

In early studies of PrP, a partially folded intermediate of PrP 90–231 has been suggested [8–10]. These partially unfolded states can potentially initiate amyloid formation [11,12]. These locally unfolded states are thermodynamically distinct from the native state, but structurally similar to it. Therefore, in addition to understanding folded structure, further understanding of intermediate PrP^{Sc} and DSE is essential. We focused on the population of the secondary structure of the DSE of huPrP under the native condition near extended conformation in this study.

In this work, the DSE of huPrP was investigated by self-guided Langevin dynamics (LD) [13,14] simulations using an all-atom point-charge force field developed by Duan et al. [15]. We have conducted a total of 25 unrestrained, independent all-atom simulations of huPrP at 300 K starting from an extended conformation. LD simulation of protein folding can easily produce millions of sets of coordinates. Clustering is a general data-mining method applied to any collection of data points where a function measuring distance between pairs of points is available. Denatured states can be categorized through such a clustering method. The structures within one cluster are ideally more similar to each other than to the structures from other clusters. From clustering analysis, the most populated structure in DSE can readily be determined. Details of the DSE were investigated and are discussed herein.

2. Methods

2.1. Simulation procedure

LD is an extended method of MD as jostling of solvent molecules causes friction, and occasionally collision perturbs the system. The local average time, the guiding factor and the collision frequency

* Corresponding author. Tel.: +886 5 2720411 66511; fax: +886 5 2722871.
E-mail address: biocil@ccu.edu.tw (C.-I. Lee).

0301-4622/$ – see front matter © 2010 Elsevier B.V. All rights reserved.
doi:10.1016/j.bpc.2010.05.002

control a self-guided LD simulation. This simulation method has an enhanced conformational search ability, and, therefore, it has been a very useful tool in macromolecule studies [13]. The generalized Born model used in this study modified the calculation of Born radii and improved the accuracy in the solvent polarization for macromolecules [16]. The combination use of the force-filed ff03 and the generalized Born model led to successful folding of several small proteins [17]. The AMBER 9.0 simulation package [18] was used in both LD simulation and data analysis. The all-atom point-charge force field (also known as ff03) built by Duan et al. [15] was applied to represent the protein. The denatured state of huPrP 121–230 was computed starting from an extended huPrP. To generate the initial extended structure, a heating method was applied to a known NMR structure (PDB code: 1hjn [19]), enabling it to unfold at 600 K for 40 ns of LD simulation to result in an extended conformation. During this simulation, the disulfide covalent bond between residues 179 and 214 was preserved. After heating huPrP, local minimization for 1000 steps was applied to minimize the resulting structure. Subsequently, the ensemble of huPrP was computed by using self-guided LD method [13] at 300 K. In total, 25 sets of self-guided LD trajectories with duration of 50 ns at 0.002 ps interval were computed based on the extended huPrP with different random number seeds to generate the initial conditions. A 16 Å force-shifted nonbonded cutoff and generalized Born solvent models with salt concentration of 0.2 M [16] were applied. A collision frequency γ of 2 ps^{-1}, guiding factor of 0.2 ps^{-1} and local sampling time of 0.2 ps for implicit solvents were used [20].

2.2. Structural analysis

The structural information of the unfolded human prion 121–230 can be illustrated as root-mean-square deviation (RMSD) of C^{α}, or radius of gyration. RMSD of C^{α} was calculated based on residues 126–227. The terminal residues in the N- and C-terminus were excluded due to their high flexibility. Radius of gyration was calculated as the root-mean-square distance of the residue from its center of gravity. The information of the secondary structure was represented by the fraction of α-helices (helicity) and anti-parallel β-strands. Native huPrP contains three helices: helices I (residues 144–156), II (residues 173–194) and III (residues 200–227) as defined by calculation with a DSSP algorithm [21]. Helicity over 50 ns of simulation was calculated based on the number of helical residues in the helix region in the denatured state as a comparison to that in the native state. The helicity of the entire huPrP was determined from residues 126 to 227. The calculation of helicity can be expressed as follows: $helicity = \frac{number\ of\ helix\ residues}{number\ of\ residues\ in\ the\ entire\ protein\ or\ in\ helix\ region}$. Similarly, the fraction of anti-parallel β-strand content was calculated. Two anti-parallel β-strand regions were defined from the native structure at residues 129–133 (β-strand I) and 160–163 (β-strand II). The fraction of anti-parallel β-strand content was calculated as $\frac{number\ of\ anti-parallel\ \beta-strand\ residues}{number\ of\ residues\ in\ the\ entire\ protein\ or\ in\ anti-parallel\ \beta-strand\ region}$.

2.3. Clustering analysis

The cluster-to-cluster distance is defined as the average of all distance between individual points of two clusters as so-called average-linkage algorithm. The average-linkage algorithm is one of the best clustering methods as suggested by Shao et al. [22] Simulated LD trajectories were clustered into distinct groups based on average-linkage methods by ptraj from the AMBER 10 simulation package [23]. Based on the main-chain RMSD, each snapshot is compared against the average coordinates of the existing groups after rigid-body alignment. A snapshot may become a member of its closest cluster if the RMSD is smaller than a given cutoff (2.5 Å). Otherwise, a new cluster would be generated if the minimum RMSD exceeded the cutoff.

3. Results and discussion

Full length huPrP is a 210-residue protein. Previous NMR study revealed that huPrP proteins contain a globular domain that extends approximately from residues 125 to 228 [24]. The N-terminal fragment of huPrP is flexibly disordered. The globular domain contains one two-stranded anti-parallel β-bridge and three α-helices. The structure of huPrP 121–230 (Fig. 1A, PDB code: 1hjn [19]) was studied in more detail. Experimental studies indicated that impairing the native protein structure is essential in fibril formation since the structural conversion of PrP protein into PrP fibrils requires denaturants [25]. The RMSD, radius gyration and the secondary structure feature of the denatured prion have not been determined experimentally. The use of strong denaturing conditions is required in experimental determination of the denatured protein structure. To gain more insight of denatured state in the native condition, computer simulation is the best solution. Therefore, we designed the extended structure as the starting structure to be compared with. After heating at 600 K, huPrP lost all characteristics of the secondary structure and turned into an extended conformation (Fig. 1B) as the starting structure of the LD simulation. The disulfide-bond between residues 179 and 214 was preserved during high-temperature simulation since previous studies indicated the existence of disulfide bonds during misfolding of PrP [26,27]. This unfolded structure was optimized by local energy minimization prior to the following LD simulations.

3.1. Analysis of RMSD of C^{α}

To quantitatively evaluate the structural similarity over the simulation time as compared to the starting huPrP native structure, RMSD of C^{α} was calculated for the globular structured region (residues 126–227). The average of 25 trajectories over 50 ns of LD simulation is illustrated in Fig. 2A. The structure of fully unfolded huPrP having mainly an extended chain conformation collapsed significantly in the initial 10 ns and the mean RMSD of C^{α} decreased from 40.1 Å to 18.0 Å. In the next 40 ns, the structure changed gradually due to partial formation of α-helices. The average trajectory indicated that the mean RMSD of C^{α} after 50 ns of LD simulation was reduced to 15.6 ± 2.0 Å. This significant decrease of RMSD of C^{α} indicated formation of compact structures.

3.2. Analysis of radius of gyration

Besides the RMSD of C^{α}, the radius of gyration of huPrP was analyzed based on 25 sets of LD trajectories. The average trajectory of the radius of gyration is shown in Fig. 2B. Similar to the trajectory of RMSD of C^{α}, the mean radius of gyration decreased extensively in the first 10 ns from 42.5 Å to 17.9 Å. Subsequently, the structure became less fluctuated in the next 40 ns. After 50 ns of LD simulation, the mean radius of gyration reached 15.9 ± 1.9 Å. Interestingly, this value is very close to mean gyration radius of native folded huPrP at 14.6 Å. The similarity between mean gyration radii indicates that denatured huPrP is not a random coil lacking inter-residue interaction but is a packed structure.

3.3. Analysis of α-helicity of native helical regions

Since the native structure of the simulated protein contains three helices, the development of the helical structure would be a good measure of the folding process. Therefore, the average of the fraction of the α-helices (helicity) of denatured huPrP was considered. Accordingly, the mean helicity averaged over 25 sets of simulations is calculated (Fig. 3A–D). The helicity of the entire PrP is only 15% (Fig. 3A). This is consistent with experimental study that PrP loses helical conformation upon structural conversion. Formation of the individual helix (Fig. 3B–D) was monitored by the

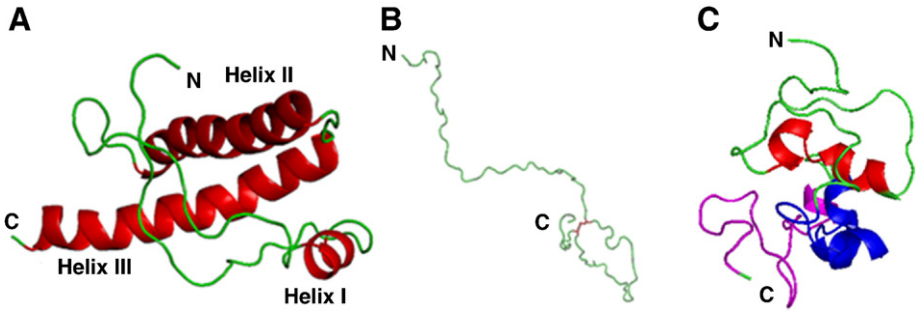

Fig. 1. (A) The NMR structure of huPrP121–231 (PDB 1hjn [19]), (B) fully unfolded huPrP 121–230 at 600 K with the disulfide-bond shown in red, and (C) the simulated denatured structure of huPrP from the most populated cluster. The helical regions I, II and III defined based on the native structure are colored in red, blue and magentas, respectively.

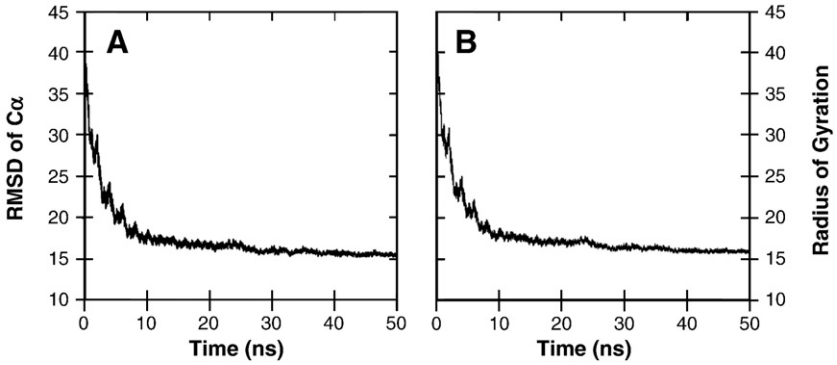

Fig. 2. The average of 25 trajectories representing (A) RMSD of C^{α} and (B) the radius of gyration of the structured region of huPrP (residues 125–228) as compared to the native huPrP structure.

development of helical content within each native helical region. The three helices performed different levels of helicity. Among the three helices, helix I formed significantly faster than the other two helix regions. Over 50 ns of simulation, helix I was 20% helical on average, while helix II and helix III were respectively 14 and 12% helical on average.

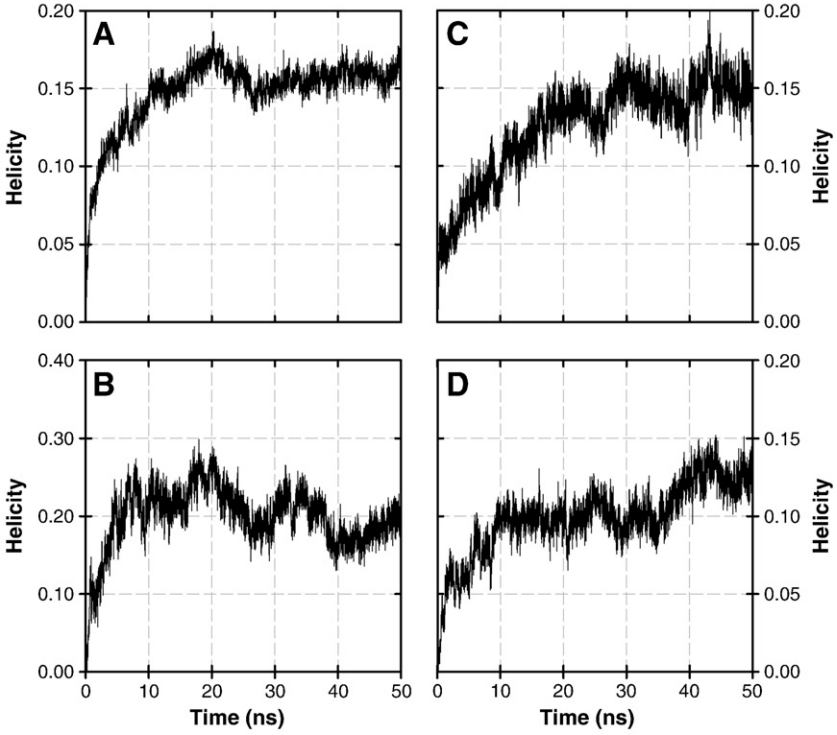

Fig. 3. The average of 25 trajectories representing the helicity in helix regions in the denatured state as a comparison to the native huPrP structure shown in (A) entire huPrP, (B) helix I, (C) helix II and (D) helix III. The helical regions are defined based on the native structure.

Among three regions of α-helices, helix I conserved the highest α-helical content. This result is consistent with a previous replica exchange molecular dynamics simulation that helix I is very stable in the sheep PrP unfolded state [28]. The sequence similarity of human and sheep PrPs is 96% based on clustal W2 algorithm [29]. Therefore, same structural features are expected on these two proteins. In the native huPrP state, helix I region has a remarkable high intrinsic helix propensity as reported by both theoretical and experimental studies [30,31]. However, a previous study incorporating the use of PrP^{Sc}-specific monoclonal antibody indicated a structural rearrangement of the sequence of helix I during the conversion reaction [32]. PrP amyloid fibrils are well recognized as β-sheet stacking. The structural rearrangement of helix I into a β-strand remains ambiguous, and more effort is needed to clarify this critical process.

The low fraction of α-helix implies that the denatured state of huPrP is not highly structured. However, the results of RMSD of C^{α} and the radius of gyration indicate that the denatured state of huPrP is a compact structure. Taking together these results of structural analysis, the denatured huPrP is between a random coil and a well-packed structure.

3.4. Analysis of anti-parallel β-strand

The significance of the formation of anti-parallel β-strand in the context of amyloid proteins is that amyloid fibrils are rich with anti-parallel β-strand structures. Therefore, we analyzed the degree of anti-parallel β-strand content using the same method as used previously for determining α-helicity. The mean fraction of β-strand averaged over 25 sets of simulation is calculated as shown in Fig. 4A–C. Formation of the individual β-strand was monitored by the development of contents featuring β-strand within the entire huPrP and in each native anti-parallel β-strand region. In the entire huPrP, the fraction of β-strand features reaches 4%. This value is much lower than α-helicity at 15%. In both anti-parallel β-strand regions, the formation of β-strand is below 3%. Differing from smooth growth of α-helix, β-strand I formed readily at 12 ns for 1%, but suddenly increased to 2% at 34 ns. Strong fluctuation was observed in β-strand II. Over 50 ns of simulation, β-strand II had not reached an equilibrium state. Lack of β-strand in DSE implies that anti-parallel β-sheets in amyloid fibrils are built from inter-molecular interactions rather than intra-molecular bonds.

3.5. Clustering analysis

Sixteen most populated clusters occupy 16.7% of analyzed snapshots. The summary of 16 clusters analyzed from 25 LD simulations is listed in Table 1. These clusters are categorized into 8 groups based on their structural features. Six clusters, including the most populated one, contain three partially formed helices. The structure from the most populated cluster (Fig. 1C) is helical at the three assigned helix regions. The helices are partially formed, which results in discontinuous helical fragments in helix I and helix II, and tiny helical fragment in helix III. In the anti-parallel β-strand region of the native state, no β-structure formed in the denatured state. Ten clusters out of 16 clusters are identified to contain partially formed helix I. This is consistent with the result of helicity analysis that helix I is dominant in the entire protein. Only one cluster does not form a significant helical structure in any of the native helical regions. Helix III does not form alone in any clusters but forms only in the company of helix II. The correlation of helix II and III is essential as the association of these two helices is linked to amyloid core of huPrP fibrils [33]. The residues in helix II are mostly involved in the amyloid core structure, while only half of residues in helix III are involved.

Table 1
Structural features of the clustering analysis of all 25 simulations.

Structural feature	No. of clusters	Occurrences (%)
Helix I only	3	3.3
Helix II only	2	1.6
Helix III only	0	0.0
Helices I and II	1	0.8
Helices I and III	0	0.0
Helices II and III	3	3.4
Helices I–III	6	6.9
No helix	1	0.7

4. Conclusion

In the present work, the denatured state of huPrP was characterized by self-guided LD simulation. The structural analysis indicated that the most populated denatured state of huPrP is partially folded with helical structures. Helix I is the most structured region, and the formation of helix III is associated with formation of helix II. Lack of β-structure suggests that β-sheets in amyloid fibrils may be formed from inter-molecular interactions rather than intra-molecular forces. Experimental observation indicated that PrP fibril is rich in β-sheet structure. This observation leads to the interpretation that helical PrP protein changed to β-structure before polymerization into fibrils. However, this study revealed that denatured state of PrP has higher content of α-helix than β-strand. Lack of structural information of denatured PrP might be the reason that PrP^{Sc} has not been explicitly identified. This structural analysis of the huPrP denatured state provides further insight into the unfolding of prion. The unfolding of prion will help us to understand the complex mechanism of protein aggregation and its role in the pathogenesis of disease.

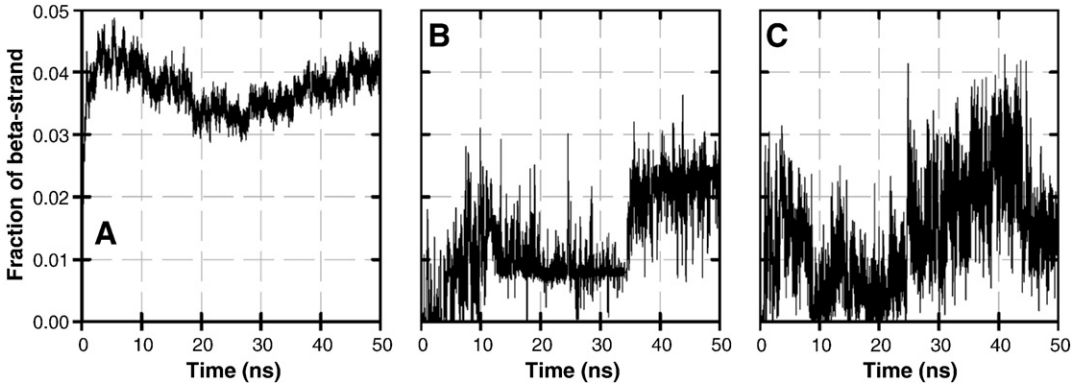

Fig. 4. The average of 25 trajectories representing the fraction of β-strand in β-bridge regions of the denatured state as a comparison to the native huPrP structure shown in (A) entire huPrP, (B) β-bridge I and (C) β-bridge II. The β-bridge regions are defined based on the native structure.

Acknowledgements

We are grateful to the National Center for High-performance Computing for computer time and facilities, and National Science Council for financial support (Project 98-2113-M-194-0003). Usage of PyMol graphics packages is gratefully acknowledged. We thank Dr. Raymond Chung for editing the manuscript. We also thank Ms. Yu-Hsin Chang and Babara Yang for their assistance on data analysis.

References

[1] D. Neri, M. Billeter, G. Wider, et al., NMR determination of residual structure in a urea-denatured protein, the 434-repressor, Science 257 (1992) 1559–1563.
[2] K. Wuthrich, NMR assignments as a basis for structural characterization of denatured states of globular proteins, Curr. Opin. Struct. Biol. 4 (1994) 93–99.
[3] D.R. Shortle, Structural analysis of non-native states of proteins by NMR methods, Curr. Opin. Struct. Biol. 6 (1996) 24–30.
[4] D. Shortle, M.S. Ackerman, Persistence of native-like topology in a denatured protein in 8 M urea, Science 293 (2001) 487–489.
[5] J. Klein-Seetharaman, M. Oikawa, S.B. Grimshaw, et al., Long-range interactions within a nonnative protein, Science 295 (2002) 1719–1722.
[6] B. Zagrovic, C.D. Snow, S. Khaliq, et al., Native-like mean structure in the unfolded ensemble of small proteins, J. Mol. Biol. 323 (2002) 153–164.
[7] S.B. Prusiner, Prions, Proc. Natl. Acad. Sci. USA 95 (1998) 13363–13383.
[8] A.C. Apetri, K. Surewicz, W.K. Surewicz, The effect of disease-associated mutations on the folding pathway of human prion protein, J. Biol. Chem. 279 (2004) 18008–18014.
[9] E.M. Nicholson, R.W. Peterson, J.M. Scholtz, A partially buried site in homologous HPr proteins is not optimized for stability, J. Mol. Biol. 321 (2002) 355–362.
[10] K. Kuwata, H. Li, H. Yamada, et al., Locally disordered conformer of the hamster prion protein: a crucial intermediate to PrPSc? Biochemistry 41 (2002) 12277–12283.
[11] F. Chiti, C.M. Dobson, Amyloid formation by globular proteins under native conditions, Nat. Chem. Biol. 5 (2009) 15–22.
[12] A. Abedini, D.P. Raleigh, A role for helical intermediates in amyloid formation by natively unfolded polypeptides? Phys. Biol. 6 (2009) 15005.
[13] X.W. Wu, B.R. Brooks, Self-guided Langevin dynamics simulation method, Chem. Phys. Lett. 381 (2003) 512–518.
[14] E.Z. Wen, M.J. Hsieh, P.A. Kollman, et al., Enhanced ab initio protein folding simulations in Poisson–Boltzmann molecular dynamics with self-guiding forces, J. Mol. Graph. Model. 22 (2004) 415–424.
[15] Y. Duan, C. Wu, S. Chowdhury, et al., A point-charge force field for molecular mechanics simulations of proteins based on condensed-phase quantum mechanical calculations, J. Comput. Chem. 24 (2003) 1999–2012.
[16] A. Onufriev, D. Bashford, D.A. Case, Exploring protein native states and large-scale conformational changes with a modified generalized born model, Proteins 55 (2004) 383–394.
[17] H. Lei, C. Wu, Z.X. Wang, et al., Folding processes of the B domain of protein A to the native state observed in all-atom ab initio folding simulations, J. Chem. Phys. 128 (2008) 235105.
[18] D.A. Case, T.A. Darden, I.T.E. Cheatham, et al., AMBER 9, University of California, San Francisco, CA, 2006.
[19] L. Calzolai, R. Zahn, Influence of pH on NMR structure and stability of the human prion protein globular domain, J. Biol. Chem. 278 (2003) 35592–35596.
[20] X.W. Wu, S.M. Wang, Enhancing systematic motion in molecular dynamics simulation, J. Chem. Phys. 110 (1999) 9401–9410.
[21] W. Kabsch, C. Sander, Dictionary of protein secondary structure: pattern recognition of hydrogen-bonded and geometrical features, Biopolymers 22 (1983) 2577–2637.
[22] J.Y. Shao, S.W. Tanner, N. Thompson, et al., Clustering molecular dynamics trajectories: 1. Characterizing the performance of different clustering algorithms, J. Chem. Theory Comput. 3 (2007) 2312–2334.
[23] D.A. Case, T.A. Darden, I.T.E. Cheatham, et al., AMBER 10, University of California, San Francisco, CA, 2008.
[24] R. Zahn, A. Liu, T. Luhrs, et al., NMR solution structure of the human prion protein, Proc. Natl Acad. Sci. USA 97 (2000) 145–150.
[25] I.V. Baskakov, G. Legname, M.A. Baldwin, et al., Pathway complexity of prion protein assembly into amyloid, J. Biol. Chem. 277 (2002) 21140–21148.
[26] E. Turk, D.B. Teplow, L.E. Hood, et al., Purification and properties of the cellular and scrapie hamster prion proteins, Eur. J. Biochem. 176 (1988) 21–30.
[27] E. Welker, L.D. Raymond, H.A. Scheraga, et al., Intramolecular versus intermolecular disulfide bonds in prion proteins, J. Biol. Chem. 277 (2002) 33477–33481.
[28] A. De Simone, A. Zagari, P. Derreumaux, Structural and hydration properties of the partially unfolded states of the prion protein, Biophys. J. 93 (2007) 1284–1292.
[29] J.D. Thompson, D.G. Higgins, T.J. Gibson, CLUSTAL W: improving the sensitivity of progressive multiple sequence alignment through sequence weighting, position-specific gap penalties and weight matrix choice, Nucleic Acids Res. 22 (1994) 4673–4680.
[30] J. Ziegler, H. Sticht, U.C. Marx, et al., CD and NMR studies of prion protein (PrP) helix 1. Novel implications for its role in the PrPC → PrPSc conversion process, J. Biol. Chem. 278 (2003) 50175–50181.
[31] M.P. Morrissey, E.I. Shakhnovich, Evidence for the role of PrP(C) helix 1 in the hydrophilic seeding of prion aggregates, Proc. Natl Acad. Sci. USA 96 (1999) 11293–11298.
[32] S. Hornemann, C. Korth, B. Oesch, et al., Recombinant full-length murine prion protein, mPrP(23–231): purification and spectroscopic characterization, FEBS Lett. 413 (1997) 277–281.
[33] X. Lu, P.L. Wintrode, W.K. Surewicz, Beta-sheet core of human prion protein amyloid fibrils as determined by hydrogen/deuterium exchange, Proc. Natl Acad. Sci. USA 104 (2007) 1510–1515.